

## FRACTAL EVALUATION OF TUMOR GROWTH MODELS

Loretta ICHIM<sup>1</sup>, Radu DOBRESCU<sup>2</sup>

**Abstract.** *The paper presents two applications of fractal analysis techniques in order to develop new software instruments for cancer research. Essentially the applications refer to two types of tumor growth models, the first in the case of avascular tumors, the second in the case of vascularized tumors. The fractal evaluation of the accuracy of tumoral growth models is discussed, with care to avoid the conflict between the real complexity of the biological process and a reductionist approach for simplest modeling.*

**Keywords:** Biological system modeling, Biomedical informatics, Cancer, Fractals, Tumor growth, Simulation

### 1. Introduction

Tumor growth is a most complex process, ultimately dependent on tumor cells proliferating and spreading in host tissues. A very important implication of the spatial and temporal symmetries of tumors is that certain universal quantities can be defined which allow the characterization of the tumor growth dynamics.

Modeling and simulation of tumor growth in competition with the immune system is certainly one of the challenging frontiers of applied mathematical which could have a great impact both on the quality of life and development of mathematical sciences. The common feature of the above mathematical approach is that the equation model living matter and the ability of cells to organize their dynamics needs to be an essential feature of these mathematical models.

Tumor evolution is a most complex process involving many different phenomena. Understanding the dynamics of cancer growth is one of the great challenges of modern science. Solid tumors develop initially as a single mass of cells. These divide more rapidly than the cells around them because of a proliferative advantage caused by mutation, and a number of genetic pathways responsible for these mutations have been identified over the last decade [1], [2].

Because there are three distinct stages (avascular, vascular, and metastatic) to cancer development, researchers often concentrate their efforts on answering specific questions on each of these stages. Nevertheless, when attempting to model any complex system it is wise to try and understand each of the components as well as possible before they are all put together.

---

<sup>1</sup>Ph.D., “Ștefan S. Nicolau” Institute of Virology, Bucharest, Romania.

<sup>2</sup>Prof., Control Systems and Industrial Informatics Dept., “Politehnica” University of Bucharest, Romania.

The avascular stage of tumor growth is characterized by small tumors, which gain the nutrients and oxygen they need for survival and growth by diffusion from external blood vessels. Since there are no blood vessels within the tumor to supply the mass needed for such volume expansion, this must also enter through the tumor's periphery.

An individual tumor cell has the potential, over successive divisions, to develop into a cluster of tumor cells. Further growth and proliferation lead to the development of an avascular tumor consisting of approximately  $10^6$  cells, which feed on oxygen and other nutrients present in the local environment.

Angiogenesis is the process, by which tumors induce blood vessels from the host tissue to sprout capillary tips, which migrate towards and ultimately penetrate the tumor, providing it with a circulating blood supply and, therefore, an almost limitless source of nutrients.

The vascular growth phase, which follows angiogenesis, is marked by a rapid increase in cell proliferation and is usually accompanied by an increase in the pressure at the center of the tumor. This may be sufficient to occlude blood vessels and, thereby, to restrict drug delivery to the tumor.

In the earliest stages of development, tumor growth seems to be regulated by direct diffusion of nutrients and wastes from and to surrounding tissue. When a tumor is very small, every cell receives nourishment by simple diffusion and the growth rate is exponential in time.

However, this stage cannot be sustained because as a nutrient is consumed its concentration must decrease towards the center of the tumor. The concentration of a vital nutrient at the center will fall below a critical level.

The main aim of this paper is to develop an accurate growth model for a better understanding of process dynamics and the developing of better techniques for the prediction of evolution in real instances of cancer.

## 2. Related Works

The process of nutrient consumption and diffusion inside tumors has been modeled since the mid 1960<sup>s</sup>. There have been several reviews ([3], [4]) of this area of tumor modeling published over the last few years. However, they all focus on different aspects to those we address.

Most models fall into two categories: *A. continuum mathematical models* that use space averaging and thus consist of partial differential equations and *B. discrete cell population models* that consider processes on the single cell scale and introduce cell-cell interaction using cellular automata type computational machinery.

### A. Continuum cell population models

Mathematical models describing continuum cell populations and their development classically consider the interactions between the cell number density and one or more chemical species that provide nutrients influence the cell cycle events of a tumor cell population. Thus these models typically consist of reaction-diffusion equations. One of the best parameterized of these models is due to [5].

Early models of nutrient-limited tumor growth calculated the nutrient concentration profiles as a function of tumor spheroid radius that was changing due to the rate of cell proliferation [6], [7]. The later models have incorporated differing degrees of complexity for cell movement. For example, cells can be considered to move in either a convective manner or actively in a diffusive manner, or in a diffusive/chemotactic manner.

Most models consider tumor cell proliferation and death to be dependent on only one generic nutrient (most often oxygen). The equations describing the distribution of molecular species inside the tumor spheroid are classical transport/mass conservation equations.

### B. Discrete cell population models

With the huge advances in biotechnology, large amounts of data on phenomena occurring on a single cell scale are now available. This, combined with *in vitro* experiments using tumor spheroids, sandwich culture, etc., and high power confocal microscopy that enables tracking of individual cells in space and time, has brought about the possibility of modeling single-cell-scale phenomena and then using the techniques of up scaling to obtain information about the large-scale phenomena of tumor growth.

There are several up scaling techniques; the most popular ones are cellular automata [8], lattice Boltzmann methods [9], agent based [10], extended Potts [11] and the stochastic (Markov chain) approach [12].

The difficulty with automaton models is realistically modeling cell motion. The first step in setting up rules for cell motion is to partition the physical space into automaton cells. The simplest partition is to discretize into a regular lattice; rectangular lattices are usually chosen for simplicity.

The second modeling decision is whether the lattice is fixed in time or varies as the elements move. It is far simpler to consider a fixed lattice, with each automaton cell corresponding to either a biological cell or vacant site, and cells able to move into a nearby lattice site containing a vacant site. In particular, while the rules of motion for fixed lattices can be formulated simply in terms of cells moving between lattice sites, if the lattice is free to move and the cells can grow.

A recent three-dimensional cellular automata model, which does not use a regular lattice, is that of [13]. The model does not include nutrients or mechanical interaction between cells explicitly, but mimics the effect of both in a phenomenological way. The authors use random fixed lattice, with the space that belongs to a single lattice site consisting of points that are nearer to this site than any other lattice site.

In this model, the proliferation is determined by the distance of the cell from the tumor boundary to mimic the effects of nutrient diffusion and consumption; only cell within a certain distance from the boundary can proliferate. Similarly, cells a certain distance from the boundary become necrotic.

### 3. Modeling methods

#### A. Application 1 – modeling avascular tumor growth

##### 1) General considerations

Mathematical modeling is an ideal approach for teasing apart mechanisms of cancer invasion because it can simultaneously and quantitatively consider interactions between multiple factors. In general, simulations may need the use of dedicated computer devices, to solve systems, which include biological variables in the various transport phenomena related to biological system. The common feature of the above mathematical approach is that the equation model living matter and the ability of cells to organize their dynamics needs to be an essential feature of these mathematical models.

The biology of tumor micro regions has been investigated experimentally using the multicell spheroid model [14], [15]. In experimental setting, the spheroids are usually initiated from aggregates consisting of several cells, but as their size increases, their growth kinetics become similar to those of tumor *in vivo*, such as micro metastases or pre-vascular primary tumors. The multicell spheroids develop layered structure with a central necrotic core surrounded by quiescent cells and a thin rim of proliferating cells. Steep gradients in oxygen, glucose and other metabolites are also observed in such spheroids.

The goal of this application was to develop a two-dimensional model to simulate the avascular tumor growth based on nutrient consumption. In the same time we discuss the fractal analysis as a morphometric measure of the irregular structures typical for tumor growth.

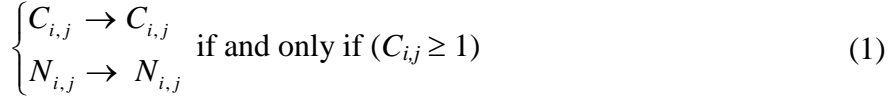
##### 2) The model

The basic principles included in the model are cell proliferation, quiescent and necrosis. Each cell has associated with the velocity, which indicates the direction and the distance the cell will move in one time step.

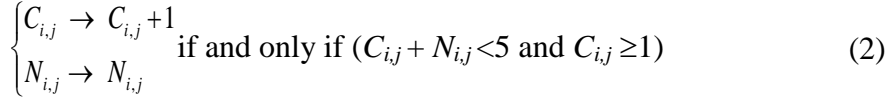
There are nine velocity channels in each lattice site:  $V_0 = (0,0)$ ,  $V_1 = (1,-1)$ ,  $V_2 = (0,1)$ ,  $V_3 = (0,-1)$ ,  $V_4 = (-1,-1)$ ,  $V_5 = (-1,0)$ ,  $V_6 = (-1,1)$ ,  $V_7 = (0,1)$ ,  $V_8 = (1,1)$ , where  $V_0$  is resting channel and  $V_1, V_2, V_3, V_4, V_5, V_6, V_7$  and  $V_8$  represent moving to right, up, left, down and diagonals, respectively. In each lattice site, we allow at most one cell (necrotic cells or tumor cells) with each velocity.

Now in each lattice site one of following reactions can occur at each time step:

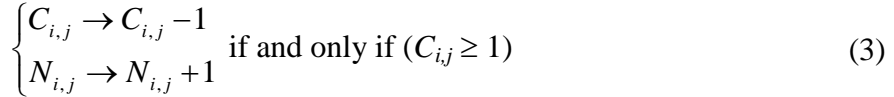
Quiescent:



Proliferation:



Necrosis:



where  $C$  – tumor cells;  $N$  – necrotic cells.

In order to address the formation of tumor micro regions, we present a two-dimensional time-dependent mathematical model in which every tumor cell is treated as an individual entity characterized by its own geometry and individually controlled cell processes. This model allows one to follow fate of each individual cell and to investigate how changes occurring in individual cells can influence behavior of the whole tumor tissue. For simplicity, we introduce in our model only one external metabolic factor and take explicitly into account only the effect of nutrient consumption on cell growth and metabolism.

Starting from the simplified discrete nutrient equation:

$$\Delta_2 N = \gamma_2 C f(N) \quad (4)$$

where  $f(N) = N$ , if  $N < 1/3$  and  $f(N) = 1$  otherwise,  $\Delta_2$  is the second numerical difference,  $C$  is 1 or 0, depending on whether a cell occupies that lattice site or not and  $\gamma_2$  is parameter of order 0.1, a scenario of a quasi-random invasion process is proposed next. Consider a  $nn \times nn$  square lattice, with possible values  $nn = 16$ ,  $nn = 32$ ,  $nn = 64$  or  $nn = 128$ . The relative nutrient  $N = n/n_\infty$  is the invading variable, called *invader*. Denote  $(i, j)$  a place in the lattice, representing a cell and consider in (4) the approximation  $\gamma_2 = 0.3$ , as specified in [16].

The discrete invader equation (4) can be rewritten, for the cell  $(i, j)$ , as:

$$N_{ij}(k+2) = 2N_{ij}(k+1) - N_{ij}(k) + 0.3C(i, j)f(N_{ij}(k)) \text{ where:} \quad (5)$$

$k$  is the discrete time,  $N_{ij}$  is the invader in the cell  $(i, j)$ ,  $f(N_{ij}(k)) = N_{ij}(k)$ , if  $N_{ij}(k) < 1/3$ ,  $f(N_{ij}(k)) = 1$  otherwise,  $C(i, j) = 1$  if the cell  $(i, j)$  is occupied by the tumour and  $C(i, j) = 0$  otherwise.

The dynamic model (5) is piecewise linear, with the right hand term depending on the values of  $f$  and  $C$ . For an occupied cell with  $N_{ij}(k) < 1/3$ , the system (5) is linear and free, with the characteristic polynomial:

$$\chi_1(\lambda) = \lambda^2 - 2\lambda + 0.7 \quad (6)$$

and the eigenvalues  $\lambda_{1,2} = 1 \pm \sqrt{3}$ , with  $|\lambda_1| > 1$ .

For  $N_{ij}(k) \geq 1/3$ , the system (5) is forced with a constant term equal to 0.3 in the right hand side and has the characteristic polynomial:

$$\chi_2(\lambda) = \lambda^2 - 2\lambda + 1 \equiv \lambda^2 + \alpha_1\lambda + \alpha_0 \quad (7)$$

with the roots  $\lambda_{1,2} = 1$ .

Assuming that the nutrient starts from the normal value  $n_\infty$ , i.e. for initial conditions in (5)  $N_{ij}(0) = N_{ij}(1) = 1 > 1/3$ , the relative nutrient grows monotonically.

In this modeling approach, the invasion process has no enemy or partner, so the process is not a game. The invasion starts from the center of the lattice, with an initial kernel of invaded cells, and at each moment  $k$ , if the invader numerical gradient reaches, in some already invaded cell, a given limit, then an unoccupied – i.e. not belonging to the tumor - or “empty” adjacent cell will be randomly invaded.

Denote *slope* a given lower bound for the invader numerical gradient enabling the invasion of a neighbor cell. The condition for an event occurrence, i.e. the invasion condition from the cell  $(i, j)$  to one of its neighbors  $(ii, jj)$  is:

$$\begin{aligned} & \text{if } \{ C(i, j) = 1 \} \wedge \{ N_{ij}(k+2) - N_{ij}(k+1) \geq \text{slope} \} \text{ then} \\ & \{ \text{generate rand}(i, j) \in (0,1) \} \wedge \{ \text{jump to } (ii, jj) = \text{Rule}(i, j, \text{rand}(i, j)) \}, \end{aligned} \quad (8)$$

mechanism for quasi-random number generation.

For the cell  $(i, j)$  in the  $nm \times nm$  lattice, with  $C(i, j) = 1$ , the pair  $(ii, jj)$  can be chosen according to the mentioned *Rule*, so that:

$$\{(ii, jj) \in \{(i, j+1), (i-1, j), (i, j-1), (i+1, j)\}\} \wedge \{C(ii, jj) = 0\} \wedge \{(1 \leq ii \leq nn) \wedge (1 \leq jj \leq nn)\}. \quad (9)$$

### 3) Modeling the invasion control as an inhibitor action

The invasion process is undesired, on one side, and unstable on the other side so it is reasonable to try to limit the unwanted invasion by means of an inhibitor, which may play the role either of an immune response, as a feedback control, or of a treatment. A natural way to build a model of the controlled invasion process is by adding a correction variable in the right-hand side of equation (5). Denote  $M_{ij}(k)$  the current inhibitor for the relative nutrient in a cell  $(i, j)$ . The controlled relative nutrient dynamics is given by:

$$N_{ij}(k+2) = 2N_{ij}(k+1) - N_{ij}(k) + 0.3C(i, j)f(N_{ij}(k)) + M_{ij}(k) \quad (10)$$

The state variables and the control in the model (10) are defined as:

$$x_1(k) = N_{ij}(k), \quad x_2(k) = N_{ij}(k+1), \quad u(k) = M_{ij}(k). \quad (11)$$

The corresponding state realization of the controlled model (10) is:

$$\begin{aligned} x_1(k+1) &= x_2(k) \\ x_2(k+1) &= -x_1(k) + 2x_2(k) + 0.3C(i, j)f(x_1(k)) + u(k) \end{aligned} \quad (12)$$

Denote  $\mathbf{x}(k) = [x_1(k) \quad x_2(k)]^T$  the state of the system (12) at the moment  $k$  and observe that, similarly to the free model (5), the controlled models (10) and (12) are piecewise-linear. In an occupied cell  $(i, j)$ , i.e. for  $C(i, j) = 1$ , if  $f(x_1(k)) = 1$ , the dynamics (12) with output  $y(k) = N_{ij}(k)$  can be written in the compact form:

$$\mathbf{x}(k+1) = \mathbf{A}\mathbf{x}(k) + \mathbf{b}(0.3 + u(k)), \quad y(k) = \mathbf{c}^T \mathbf{x}(k) + du(k) \quad (13)$$

with

$$\mathbf{A} = \begin{bmatrix} 0 & 1 \\ -1 & 2 \end{bmatrix}, \quad \mathbf{b} = \begin{bmatrix} 0 \\ 1 \end{bmatrix}, \quad \mathbf{c}^T = [1 \quad 0], \quad d = [0]. \quad (14)$$

The characteristic polynomial of the matrix  $\mathbf{A}$  is  $\chi_2(\lambda) = \det[\lambda\mathbf{I} - \mathbf{A}]$  specified in (7). The linear system  $(\mathbf{A}, \mathbf{b}, \mathbf{c}^T, d)$  with the input  $\tilde{u}(k) = 0.3 + u(k)$ ,  $k = 0, 1, 2, \dots$ , is controllable so, according to the classical control theory, the closed loop evolution can become asymptotically stable by a feedback control  $\tilde{u}(k) = \tilde{\mathbf{f}}^T \mathbf{x}(k)$ , with  $\tilde{\mathbf{f}}^T = [\tilde{f}_1 \quad \tilde{f}_2] \in \mathbf{R}^{1 \times 2}$  chosen so that the characteristic polynomial  $\det[\lambda\mathbf{I} - (\mathbf{A} + \mathbf{b}\tilde{\mathbf{f}}^T)]$  equals some desired polynomial:

$$\chi_0(\lambda) = \lambda^2 + \beta_1\lambda + \beta_0 = (\lambda - \lambda_{i0})(\lambda - \lambda_{20}), \quad \beta_0, \beta_1 \in \mathbf{R}, \quad (15)$$

with  $|\lambda_{i0}| < 1$ ,  $i = 1, 2$ .

The proposed control problem for the system (12) is slightly different: the objective is to bring, in each cell, the relative nutrient to  $1 = \lim_{k \rightarrow \infty} N(k)$ , for which the nutrient equals the “normal” value  $n = n_\infty$  and also to admit that there might appear a delay in the inhibitor action.

The speed of the transition to the desired nutrient value is imposed by the stable roots of a given polynomial  $\chi_0$  (15).

## B. Application 2 – modeling vascular tumor networks

### 1) General considerations

In the first stages of vascularization, the new vessels are not fully formed. In addition, the rate of vascularization may vary significantly between tumors.

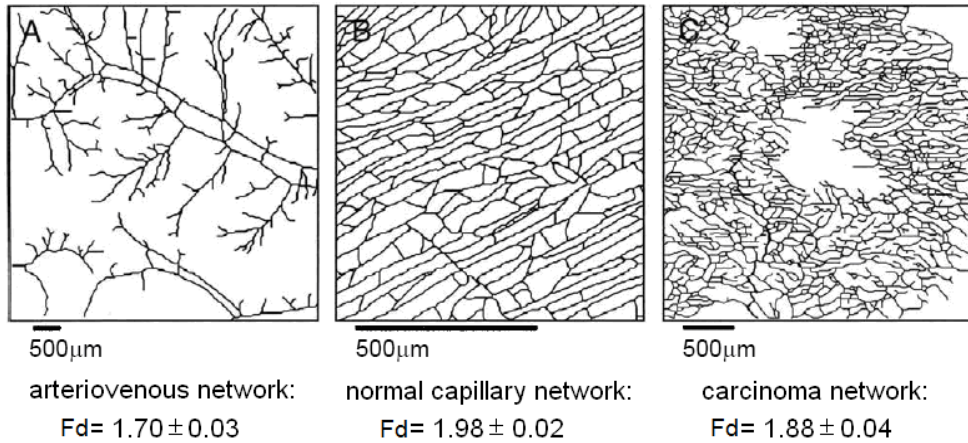


**Fig. 1.** Fractal structure of tumor vessel networks.

Taking into account that tumor size in the vascular phase of tumor growth is directly dependent on the level of vascularization, it was decided to study tumors of comparable sizes (approximately 4 mm in diameter).

Therefore, in tumors the fractal dimension (Fd) was measured for all observed vessels taken together.

In figure 1, we present the real networks and the models based on them – adapted from [17].

Fractal dimensions were estimated by the box-counting technique [18] where the fractal dimension is given by the gradient of the graph of ‘log (box size)’ against ‘log (number of boxes required to cover the image)’.

## 2) *The model*

The computer model of the vascular network starts with a square lattice, invasion percolation is implemented by first assigning uniformly distributed random values to each point on the lattice. An arbitrary start point is selected as the left bottom corner and invades the weakest point the grid at adjacent to the current network after each time point; this growth is iterated until the required occupancy is reached.

The network is then pruned by removing regions with zero flow (dead ends) to provide the 'backbone', blood vessels are then assumed to connect all adjacent lattice sites on this backbone. Selecting the occupancy enables the level of geometrical heterogeneity to be controlled as measured by the fractal dimension. This model helped to explain why tumor vascular resistance is higher than observed in normal vasculature. A foreseeable limitation of this system is fractal scaling only applies over a narrow range of length scales and it is not known if the scaling extends to larger vessels.

## 4. Experimental Results

For all applications, the models were implemented using Java Development Toolkit and the algorithms for computing fractal dimensions were implemented in Microsoft Visual C++ 6.0 software.

### A. *Application 1*

#### 1) *Simulation results*

The simulations conducted on a  $100 \times 100$  square lattice with central site initially defined to contain one cancerous cell. This simulation has been greatly simplified by neglecting some effects such as: interaction of healthy cells with cancerous cells, the effect of nutrients concentrations and limited volume space for tumor and it seems the addition of these effects is not problematic in this simulation (Fig. 2).

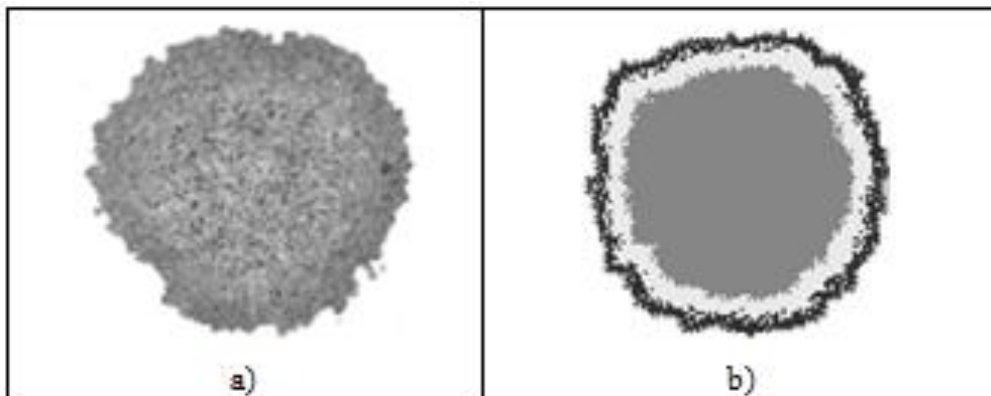


**Fig. 2.** In vitro growth model versus simulation in two dimensions.

Finally, we shall compare the simulated patterns with an *in vitro* model of tumor growth [19] for validation our computational model. In figure 2 we show two sections of tumor growth: left panel (a) – *in vitro* model and right panel (b) – simulated pattern. This image is very similar to the patterns exhibited in our simulation. At the beginning, we assume that similarities between these *in vitro* growth model and simulated patterns suggest that some of the functional properties of cancer cells are similar to those built into our model.

The size of the lattice is chosen sufficiently large such that the boundaries do not influence the tumor growth within the considered time interval. Our model estimated fast expansion of tumor cells during the first third of the whole period and significant reduction in tumor growth after developing necrotic cell area. Finally, the tumor enters into a phase of growth saturation. The percentage of proliferating tumor cells is equal to 100% during this time, except of the scattered single points that reflect short periods of time, when the newly created daughter cells did not yet enter in the new cell cycle. A subpopulation of quiescent cells becomes more noticeable at the time when the first necrotic cells arise. After subpopulation of necrotic cells arisen the tumor growth is characterized by a fast exponential expansion. The percentage of proliferating cells starts to decrease with the increasing subpopulations of quiescent and necrotic cells. Three hundred and sixty images were automatically generated for each model of tumor growth, and their fractal dimensions were estimated using box-counting method.

## 2) Computing fractal dimensions

To measure the fractal dimension and roughness of the tumor boundary we select only the cells at the boundary of the tumors.

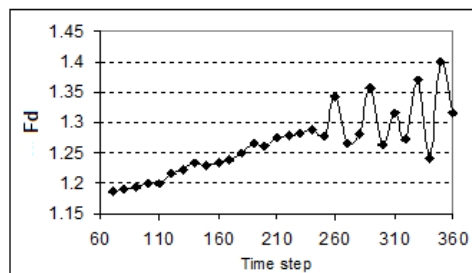


**Fig. 3.** Plot of the fractal dimensions of the tumor boundary as a function of time steps.

We define boundary cells as those that have at least one normal neighbor. Fractal dimensions were calculated using a box-counting algorithm [18]. See the figure 3 where the fractal dimensions of the patterns are plotted against the total number of time steps. We noticed that the invasive growth is afterwards slowed down while the tumor pattern became progressively more compact. This makes us suppose that it could be diagnosed in a precocious way the cancer, being based on the quantification of the fractal dimension.

## A. Application 2

### 1) Simulation results

We have developed a computer model based on invasion percolation growth process to simulate the geometrical complexity of a tumor vascular network. We used the fractal dimension as a quantitative estimator of the spatial complexity of the two-dimensional vascular network. Below are some examples of invasion percolation clusters in different sizes, with different boundary conditions (Fig. 4).

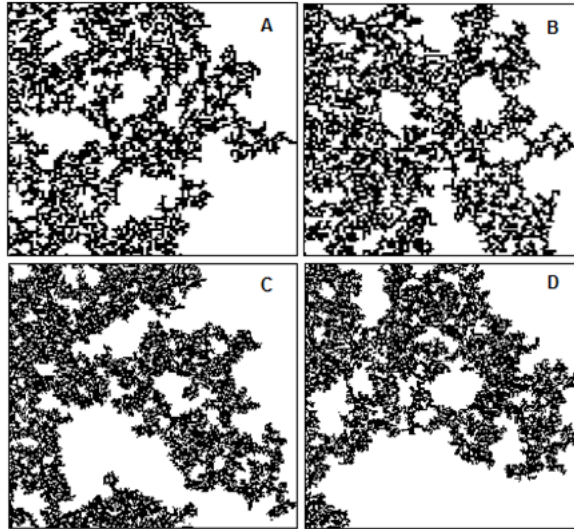


**Fig. 4.** Examples of invasion percolation clusters in different sizes and with different conditions:

- (A) a  $100 \times 100$  cluster with periodic boundary conditions and  $Fd = 1.9135$ ;
- (B) a  $100 \times 100$  cluster with free boundary conditions and  $Fd = 1.9313$ ;
- (C) a  $200 \times 200$  cluster with periodic boundary conditions and  $Fd = 1.9369$ ;
- (D) a  $200 \times 200$  cluster with free boundary conditions and  $Fd = 1.9434$ .

### 2) Computing fractal dimensions

All images were automatically generated and their fractal dimensions were estimated. The following table (table 1) includes the average fractal dimension of each type of cluster. The average is over 10 runs with different random seeds. All of the data are expressed as average fractal dimension  $\pm$  standard deviation.

**Table 1.** The average and standard deviation for  $Fd$  in different lattice and boundary conditions

| Boundary Condition | Lattice          | Average Fractal Dimension |
|--------------------|------------------|---------------------------|
| Free               | $100 \times 100$ | $1.92 \pm 0.02$           |
| Periodic           | $100 \times 100$ | $1.93 \pm 0.02$           |
| Free               | $200 \times 200$ | $1.94 \pm 0.01$           |
| Periodic           | $200 \times 200$ | $1.935 \pm 0.02$          |

## 5. Conclusions

We see the role of mathematical modeling in cancer biology as twofold.

Models can help our intuition, provide a framework for thinking about the problem, and make predictions.

If a model is well parameterized then these predictions can be quantitative predictions can be significant.

**1.** The proposed abstract invasion model inherits the lattice structure from model, but considers only the second-order discrete-time invader equation [20].

The simulated evolution of the free invasion process depends strongly on the choice of the limit slope.

On the other side, experiments performed with constant slope value have revealed a rather weak evolution variation if the initial conditions are chosen below or above the limit  $1/3$ , respectively, for which the characteristic polynomial changes from (6) to (7).

In the proposed controlled model, the correction agent is a growth inhibitor and the controlled evolution may reach a stationary state, provided that the inhibition is efficient, with the price of an increased complexity.

The discrete-time approach ensures that for both free and controlled models, the numerical simulation is non-blocking and the Zeno phenomenon is avoided.

In future research, the simple free invasion model can be developed with different transition mechanisms, implemented, in (8), by the function Rule.

Also, simulation of invasion processes in which two or several initial kernels fuse gradually, forming a single bigger tumor, may present interest.

Finally, one can extend the research from this discrete abstraction to a general network, thus renouncing to the constraints of a regular lattice.

**2.** These results confirm that its whole architecture plays a primary role in the quantitative evaluation of the vascular network.

Therefore, we consider that at the moment to validate our model is necessary systematic comparison between the computer simulations and the real data.

However, both normal and tumor vasculature can more properly be considered *fractal objects* because of their irregular shape (*spatial conformation*), self-similar structure, non-integer dimension and dependence on the scale of observation (*scaling effect*).

There are many directions in which this work will be taken in the future.

In the first research line, we are planning to investigate the transport of diffusible substances in tumors, a key process in the growth and treatment of solid tumors.

For example, adequate oxygen supply is critical for tumor growth but also for successful radiation therapy.

The scale-invariant behavior of vascular networks leads to important insights about the transport characteristics of tumors.

The inherent limitations to oxygen transport in tumor tissues having percolation-like vascular networks can be generalized to include most other substances that are delivered to target cells by similar convective and diffusive processes.

Such substances include both nutrients (e.g., glucose) and therapeutic agents (e.g., drugs).

The next line can be, for example, to extend model of invasion percolation in three-dimensional lattice.

## REFERENCES

- [1] *D. Grander*. *Medical Oncol.*, 15:20–26, 1998.
- [2] *R.A. Weinberg*. *Science*, 254:1138–1146, 1991.
- [3] *J.A. Adam*. *Invasion and Metastasis*, 16:247–267, 1996.
- [4] *R.P. Araujo, and D.L.S. McElwain*. *Bull. Math. Biol.*, 66:1039–1091, 2004.
- [5] *J.J. Casciari, S.V. Sotirchos, and R.M. Sutherland*. *Cell Proliferation*, 25:1–22, 1992.
- [6] *H.P. Greenspan*. *J. Theor. Biol.*, 56:229–242, 1975.
- [7] *J.A. Adam, and S.A. Maggelakis*. *Mathematical Biosciences*, 97:121–136, 1989.
- [8] *T. Alarcon, H.M. Byrne, and P.K. Maini*. *J. Theor. Biol.*, 225:257–274, 2003.
- [9] *N. Bellomo, and L. Preziosi*. *Math. Comput. Modell.*, 32:413–452, 2000.
- [10] *Y. Mansury*. *J. Theor. Biol.*, 219:343–370, 2002.
- [11] *E.L. Stott*. *Math. Comput. Modell.*, 30:183–198, 1999.
- [12] *W.Y. Chen, P.R. Annamreddy, and L.T. Fan*. *J. Theor. Biol.*, 221: 205–227, 2003.
- [13] *A.R. Kansal, S. Torquato, G.R. Harsh, E.A. Chiocca, and T.S. Deisboeck*. *J. Theor. Biol.*, 203:367–382, 2000.
- [14] *W. Mueller-Klieser*. *Am. J. Physiol.*, 273:1109–1123, Oct. 1997.
- [15] *R.M. Sutherland*. *Science*, 240:177–184, Apr. 1988.
- [16] *L.M. Sander, and Th.S. Deisboeck*. *Physical Review*, E66 051901, 2002.
- [17] *J.W. Baish, Y. Gazit, D.A. Berk, M. Nozue, L.T. Baxter, and R.K. Jain*. *Microvasc. Res.*, 51:327–346, 1996
- [18] *A. Bunde, and S. Havlin*. *Fractals in Science*, 1–25, 2004.
- [19] *P. Yu, M. Mustata, L. Peng, J.J. Turek, M.R. Melloch, P.M.W. French, and D.D. Nolte*. *Applied Optics*, 43:4862–4873, 2004.
- [20] *V.E. Oltean, R. Dobrescu, and L. Ichim*. *Revue Roumaine des Sciences Techniques - Serie Electrotechnique et Energétique*, 56:109–118, 2011.